Plasma Science and Technology

PAPER

Experimental study of a porous electrospray thruster with different number of emitter-strips

To cite this article: Hanwu JIA *et al* 2021 *Plasma Sci. Technol.* **23** 104003

Plasma Sci. Technol. **23** (2021) 104003 (7pp) https://doi.org/10.1088/2058-6272/ac1783

Experimental study of a porous electrospray thruster with different number of emitter-strips

Hanwu JIA (贾翰武)[1], **Maolin CHEN** (陈茂林)[1], **Xuhui LIU** (刘旭辉)[2], **Chong CHEN** (陈冲)[1], **Haohao ZHOU** (周浩浩)[3], **Hao ZHAO** (赵豪)[1] and **Zhicong HAN** (韩志聪)[1]

[1] Combustion, Internal Flow and Thermal-Structure Laboratory, Northwestern Polytechnical University, Xi'an 710072, People's Republic of China
[2] Beijing institute of Control Engineering, Beijing 100190, People's Republic of China
[3] Aircraft Design Institute of AVIC, Xi'an 710089, People's Republic of China

E-mail: chenmaolin@nwpu.edu.cn

Received 29 April 2021, revised 23 July 2021
Accepted for publication 25 July 2021
Published 27 August 2021

Abstract

The electrospray thruster is becoming popular in space propulsion due to its low power and high specific impulse. Before this work, an electrospray thruster based on a porous emitter was developed. In order to achieve larger and more stable thrust, the thruster was redesigned, and the influence of the space between strips on thrust was studied. Four types of emitter were tested, and they had 1, 3, 4 and 14 emitter-strips on the emission surface of the same size respectively. According to the experimental results, the maximum extraction voltage and emission current of the four thrusters are different under stable operational conditions. The measured stable emission currents and extraction voltages were -500 μA/-5000 V, -1570 μA/-3800 V, -1200 μA/-3800 V, and -650 μA/-4500 V, respectively. Increasing the number of strips may not result in the emission current increasing, but changing the stable operational range of the emission current per strip and the extraction voltage. The maximum stable operational extraction voltages of 3 and 4 emitter-strips are lower than those of 1 and 14 emitter-strips, but the emission currents are higher than those of 1 and 14 emitter-strips. Time-of-flight mass spectrometry was used to analyze the mass distribution and obtain the performance of the thruster in the case of thrusters with 1 and 3 emitter-strips. Both of their plumes were composed of very small ion cluster (the pure-ion regime), and their thrusts were 80.1 μN, 219.2 μN with specific impulses of 5774 s, 5047 s, respectively.

Keywords: electrospray thruster, TOF, ionic liquid

(Some figures may appear in colour only in the online journal)

1. Introduction

Electrospray thrusters are developing rapidly. They are expected to fill the technological gap in the field of micro-propulsion. The thruster emits ions or droplets from the emitter tip to generate thrust (the phenomenon of electrospray [1]). It is applied an electric field between the emitter and extractor (the structure in figure 1), and ionic liquids in emitter are subjected to electrostatic force. In addition, ionic liquids have surface tension. The electric field force and surface tension will form a balance. When the applied electric field intensity reaches the Rayleigh limit [2], this balance will be broken, and the surface of liquids will become unstable and elliptical. The bulge of the liquid surface instantly is changed into a Taylor cone [3], and a spray-like structure is formed at the tip of the cone, therefore, the electrospray thruster emits ions or droplets from the tip of the cone. There are two main emitters of porous electrospray thrusters: one is

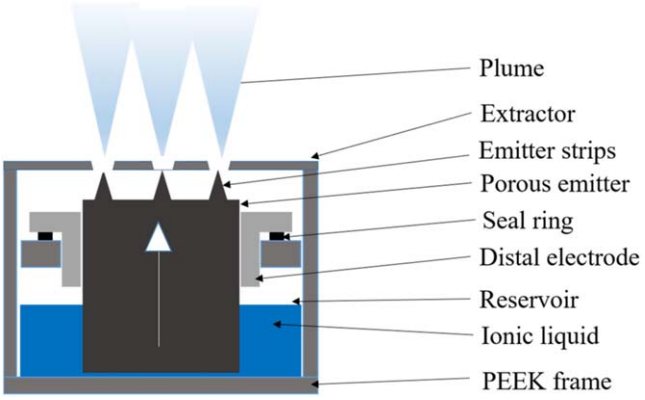

Figure 1. Structure of the electrospray thruster.

to process multiple needles on the surface of emitter, and ionic liquids of each needle are emitted in a strong electric field, the other is to process multiple parallel emitter-strips on the surface of emitter, and each emitter-strip forms multiple Taylor cones to emit. The first type of the thruster is mainly studied by the following scholars. Lozano *et al* [4–12] of the Massachusetts Institute of Technology processed 480 single modules of the emitter array on a 1 cm^2 porous glass material. When the operational voltage was 1 kV with power of 0.15 W, the thruster could output thrust of 12.5 μN with emission current of 150 μA, and specific impulse was 760 s. Ryan *et al* [13] used methods of CNC to manufacture porous ionic liquid electrospray thrusters which were PET-25 and PET-100, and thrusts of them could achieve 166 μN and 223 μN, respectively. The second type of the thruster is mainly studied by the following scholars. Mitterauer [14] explored the emission site distribution of slit emitters. Marcuccio *et al* [15] tested a linear slit field emission electric propulsion (FEEP) thruster with BMIM-Tf_2N as the propellant, and estimated the maximum thrust at 20 μN in the positive mode and 150 μN in the negative mode. And then they [16] tested the ionic liquid FEEP thruster, and confirmed that the thruster operates in pure ionic mode with a very high specific impulse. Courtney *et al* [17] prepared a porous electrospray thruster of a linear array. When emitting 1-ethyl-3-methylimidazolium-tetrafluoroborate ($EMIBF_4$), the thruster can output the thrust of 7–25 μN at input power from 0.2 to 0.7 W. Busek's [18, 19] thruster of BET300-P can generate more than 150 μN of thrust, and the specific impulse was 840–1050 s. Chen *et al* [20, 21] designed and developed a passive liquid-supply electrospray thruster that can achieve thrust of 67.1 μN, and specific impulse was 3117 s in the negative bias.

Before this study, there was an electrospray thruster that can generate thrust of 67.1 μN [20]. In order to achieve a larger and more stable thrust, a porous electrospray thruster was redesigned on the basis of the thruster, then volt-ampere characteristic tests of the thruster with different emitter-strips were carried out. Furthermore, time-of-flight (TOF) was used to analyze the mass distribution and obtain the performance in the case of thrusters with 1 and 3 emitter-strips. The experimental content is described in detail in section 4.

2. Thruster description

The structure is shown in figure 1. The thruster consists of an emitter made of porous alumina ceramics, and the specification of the emitter is a cylinder with a diameter of 31 mm and a thickness of 30 mm. Four types of emitter, which have 1, 3, 4 and 14 emitter-strips on the emission surface of same size respectively, are designed, and the emitter is mounted on the distal electrode. The height of the emitter-strips is 600 μm. Ionic liquids (1-ethyl-3-methylimidazolium-tetrafluoroborate, $EMIBF_4$) are stored in the reservoir. A polyaryletheretherketone (PEEK) frame is used as a shell. Figure 2 gives photographs of the thruster.

3. Experimental system and methods

All experiments are carried out in a vacuum environment. The pressure can reach 1×10^{-3} Pa. The test system consists of a signal generator (VC2000, VICTOR, Shenzhen, China), a pulse generator (PVX-4140, DEI Scientific, Fort Collins, CO, USA), a DC HV source (HB-S502-10AC, Hengbo, Ningbo, China), a Faraday cup, an amplifier (DHPCA-100, FEMTO, Berlin, Germany), and an oscilloscope (UTD2102CEX, UNI-T, Dongguan, China). The signal generator is used to generate voltage waveforms, which is inputted to pulse generator. The pulse generator is used to provide a pulse-shaped extraction voltage to the thruster under the supply of the DC HV source. The Faraday cup is used to collect charged particles in the plume. The amplifier is used to amplify the acquisition signals. The oscilloscope is used to observe acquisition signals. The flight distance is 34 cm, and the frequency of the pulse generator is set at 0.1 Hz in experiment. The thruster could not obtain a high emission current under positive extraction voltage in this test. The pressure in the vacuum environment is much lower than the pressure needed for gas discharge, but the pressure around the thruster is higher than 1×10^{-3} Pa, which makes the thruster form a corona. The positive corona is easier to form than the negative corona, so the thruster cannot get a high emission current under the positive extraction voltage. Therefore, the data in this work are all carried out in negative bias. Figure 3 shows a schematic diagram of the experimental system.

3.1. Volt-ampere characteristics

During the vacuum experiment, the extraction voltage of the thruster is supplied by the DC HV source. The emitter is connected to the source, and the extractor was grounded. By adjusting voltage of the source, the extraction voltage and emission current of emitter are read on the screen of the source directly.

3.2. TOF tests

TOF is one of the most effective methods to measure the mass distribution of plumes and obtain the performance of thrusters. When the pulse generator is at a high potential, charged

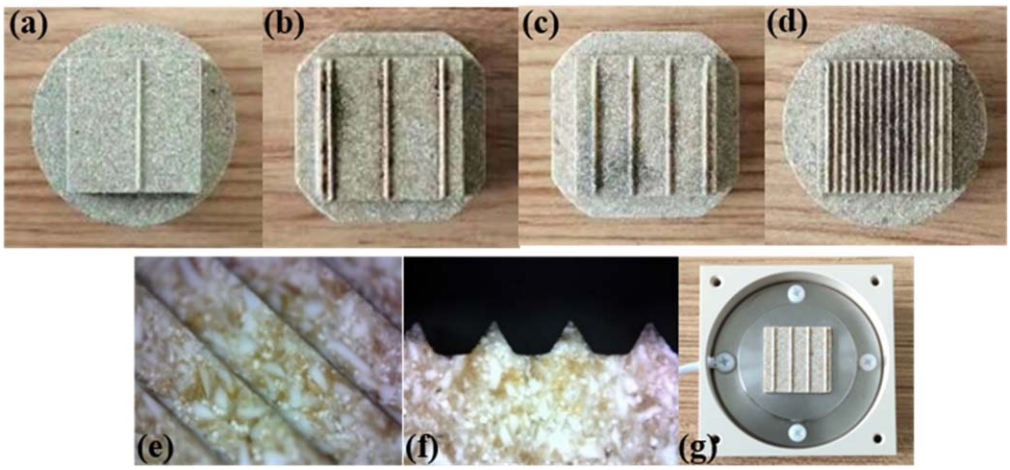

Figure 2. The thruster. 1 (a), 3 (b), 4 (c), 14 (d) emitter-strips, photomicrographs (e) and (f) of emitter-strips, and (g) the thruster.

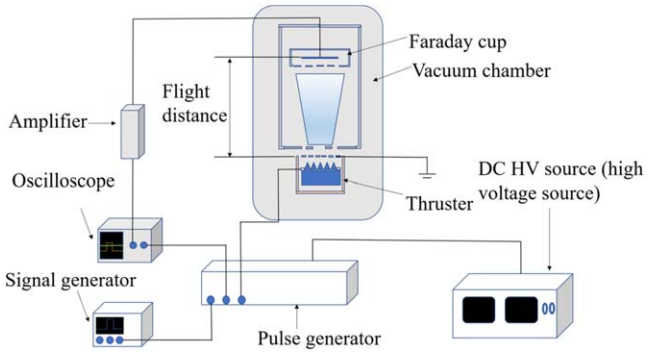

Figure 3. Experimental system.

particles in plumes can pass the flight length ($L = 34$ cm) and fly to the Faraday cup. The emission current at this time is the total emission current. When the pulse generator is at a low potential, the source of charged particles is cut off. The charged particles that have been emitted have different flight speeds due to the difference in charge-to-mass ratio. Different charged particles reach the Faraday cup successively. After the thruster is turned off, charged particles collected by the Faraday cup gradually decrease with obvious steps which correspond to BF_4^- (the first step of the TOF curve), $(EMI-BF_4)BF_4^-$ (the second step of the TOF curve), and polymers (the third step of the TOF curve). Therefore, the plume composition could be calculated with TOF curves. In order to express the proportion of each component conveniently, $n = 0$, $n = 1$, and $n > 1$ represent the proportion of BF_4^-, $(EMI-BF_4)BF_4^-$, and polymers $((EMI-BF_4)_nBF_4^-$, $n \geq 2)$ respectively.

3.3. Calculation of specific impulse and thrust

The composition of thruster 's plumes is obtained by TOF, then its thrust, specific impulse and other parameters could be calculated. Assuming that the acceleration voltage of a charged particle is equal to the extraction voltage, and all electrical energy is converted into the kinetic energy of the particle. According to the conservation of energy, we can get:

$$Uq = \frac{1}{2}mv^2, \tag{1}$$

where q, m, v and U denote the charge quantity, mass, velocity of the charged particle, and the voltage of emitter.

In the TOF experiment, the flying speed of the charged particle in the plume can be obtained according to the following formula:

$$v = \frac{L}{t}, \tag{2}$$

where L denotes the distance between the thruster and the Faraday cup, and t denotes the flight time of the charged particle.

According to the following formulas, the mass flow rate, thrust and specific impulse of the thruster can be calculated:

$$\dot{m} = \frac{2U}{L^2}\int_{t_0}^{t_{\mathrm{TOF}}} \left|\frac{\mathrm{d}I}{\mathrm{d}t}\right| t^2 \mathrm{d}t, \tag{3}$$

$$T = \frac{2U}{L}\int_{t_0}^{t_{\mathrm{TOF}}} \left|\frac{\mathrm{d}I}{\mathrm{d}t}\right| t\mathrm{d}t, \tag{4}$$

$$I_{\mathrm{sp}} = \frac{T_{\mathrm{TOF}}}{g\dot{m}}, \tag{5}$$

where $\dot{m}$ denotes the mass flow rate, t_0 denotes the initial time of TOF, t_{TOF} denotes the time when the emission current signal decreased to 0, $\frac{\mathrm{d}I}{\mathrm{d}t}$ denotes the rate of emission current change when charged particles hit the Faraday cup, I_{sp} denotes specific impulse of the thruster, and g denotes the gravitational acceleration.

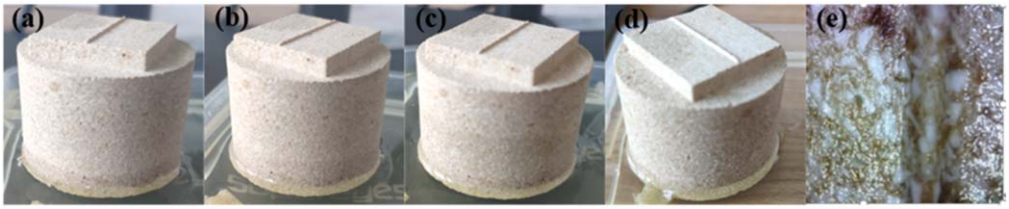

Figure 4. (a)–(d) Adsorption of ionic liquids, and (e) photomicrograph of the emitter-strip.

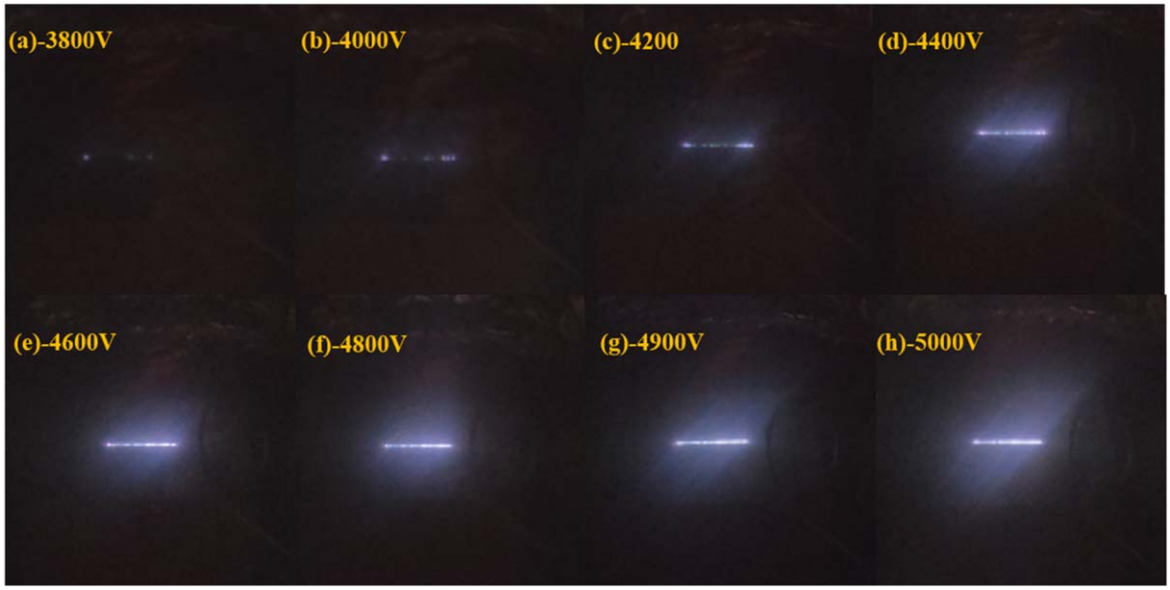

Figure 5. Ignition diagrams of 1 strip thruster.

4. Results and discussion

4.1. Ignition experiments of 1 emitter-strip thruster

Figures 4(a)–(d) show adsorption effect of the emitter on the ionic liquids, and the emitter is left for 6, 14, 43, and 107 min later, respectively. Figure 4(e) is a photomicrograph of the emitter tip.

Figure 5 shows ignition photos of the thruster with 1 emitter-strip at different extraction voltages. As the extraction voltage increased, the emitter was gradually lit, and the light intensity reached the maximum at −5000 V. The 1 strip thruster with high emission current operated stably.

In order to obtain thrust and specific impulse of the thruster, the plume compositions were analyzed by TOF. Because the maximum voltage of the pulse generator was 3500 V, the voltage of all TOF experiments was less than 3500 V. Figure 6 shows TOF curves at different extraction voltages, and it can be seen that there were two obvious steps which were BF_4^- and $(EMI-BF_4)BF_4^-$ respectively. In addition, there were noise signals in the figure, because the frequency of noise signals is much higher than the falling edge signals of TOF, noise signals can be filtered out, and it did not affect the accuracy of composition analysis. In figure 7, the obtained mass distribution of thruster's plumes according to TOF is shown.

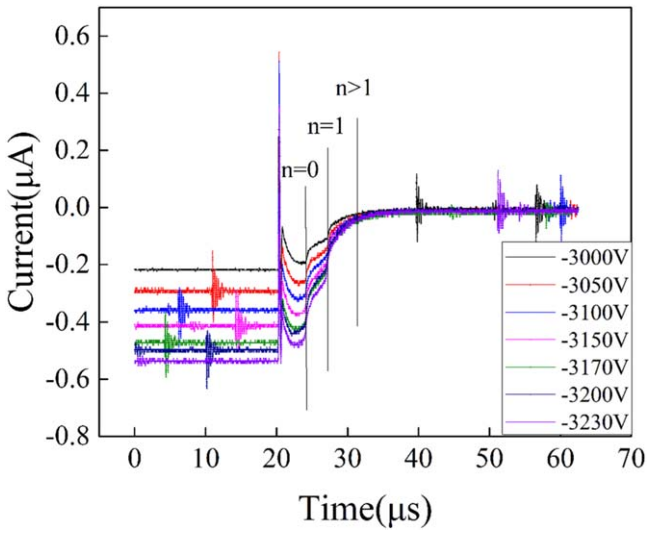

Figure 6. TOF data with 1 emitter-strip at different extraction voltages.

As displayed in figure 7, the proportions of $n = 0$ (BF_4^-), $n = 1$ ($(EMI-BF_4)BF_4^-$), and $n > 1$ (polymers) at different extraction voltages were 33.65%–37.53%, 35.51%–39.26%, and 25.32%–29.55%, respectively. From these results,

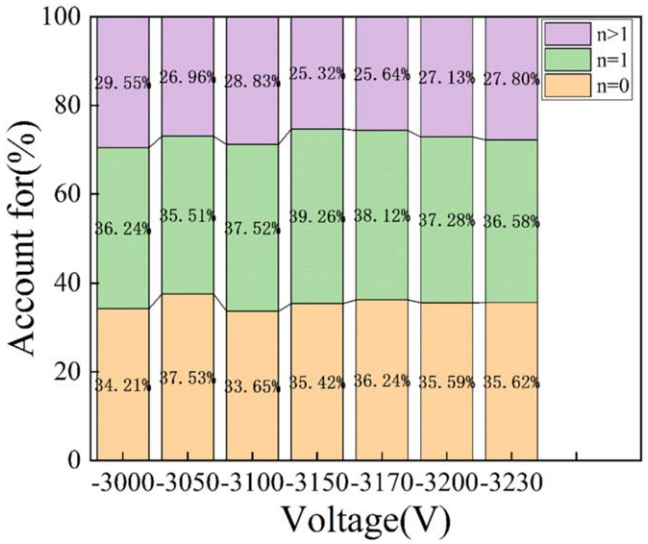

Figure 7. Proportion of plume components with 1 emitter-strip.

Table 1. The average proportion of each ion cluster in the plumes with 1 emitter-strip.

Propellant	$(EMI-BF_4)_nBF_4^-$		
Number of molecules	$n=0$	$n=1$	$n>1$
Average proportion (%)	35.47	37.21	27.32

changes of extraction voltage had little effect on plume compositions, with table 1 showing the average composition according to figure 7. It can be seen from table 1 that plumes were mainly pure ions and ion clusters with 1 molecule (accounting for 72.68%), so the thruster can obtain better performance.

According to the average composition in table 1, specific impulse and thrust are shown at different extraction voltages in figure 8. The thrust ranges of the thruster were 0.52–80.1 μN with specific impulse of 4691–5774 s at −3300 to −5000 V. The specific impulse increased as extraction voltage increased. Firstly, the thrust and emission current increased exponentially, followed by linear increase. The emission current can reach −500 μA at −5000 V, and the operational state was very stable. When extraction voltage continued to increase, the operational state was particularly unstable.

4.2. Ignition experiments of multi-strip thrusters

Three kinds of multi-strip thrusters were tested, and they had 3, 4 and 14 parallel emitter-strips, respectively. These emitters used same raw material. Figures 9(a)–(c) show ignitions of 3, 4, and 14 emitter-strips, respectively. When extraction voltages were −3800 V (a), −3800 V (b), and −4500 V (c), the emission currents were as high as −1570, −1200 and −650 μA, respectively, and the emission currents of 3 and 4 emitter-strips were very stable. As extraction voltage continued to increase, the

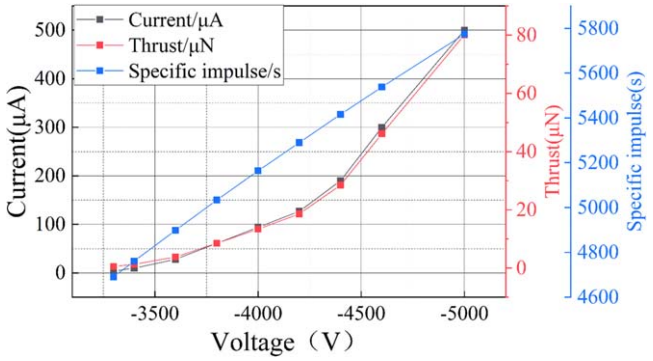

Figure 8. Emission current, thrust and specific impulse with 1 emitter-strip.

operational state was particularly unstable. Figure 9(a) showed that the thruster's each emitter-strip was fully lit, but figures 9(b) and (c) showed that the two thrusters' emitter-strips were not fully lit. It could be inferred that the electric fields between the strips would interfere with each other in the state of thruster ignitions.

From experiments, the operational state of the thruster with 3 emitter-strips was the most stable, therefore, the variation of emission current at different extraction voltages was measured, and the plume compositions were analyzed. Figure 10 shows TOF curves at different extraction voltages, and it can be seen that there are two obvious steps which are BF_4^- and $(EMI-BF_4)BF_4^-$, respectively. The curves of TOF were similar to the 1 strip thruster.

Figure 11(a) shows the total emission current of two thrusters with 3 emitter-strips and 4 emitter-strips. Both thrusters have a maximum emission current value at −3800 V. When the extraction voltage is higher than −3800 V, both thrusters began to discharge. The total emission current of the 3 emitter-strips is similar to that of the 4 emitter-strips when the extraction voltage is below −3300 V, and a little higher than that of the 4 emitter-strips when the extraction voltage is above −3300 V. For more details, figure 11(b) presents the emission current per strip of these two thrusters at different extraction voltages. It can be seen that the emission current per strip of the 3 emitter-strips is much higher than that of the 4 emitter-strips under the same extraction voltage. With the extraction voltage increasing, the difference of emission current per strip between these two thrusters grows ever greater.

It can be seen from figure 12 that the proportions of $n=0$ (BF_4^-), $n=1$ $((EMI-BF_4)BF_4^-)$ and $n>1$ (polymers) at different extraction voltages were 34.24%–36.28%, 35.35%–39.27% and 26.49%–28.58%, respectively. Proportions were similar with that of 1 strip thruster, and the changes in extraction voltage had little effect on plume compositions. Table 2 shows average composition according to figure 12. It can be seen from table 2 that plumes were composed mainly by pure ions and ion clusters with 1 molecule (accounting for 72.51%), so the thruster can achieve better performance (thrust and specific impulse).

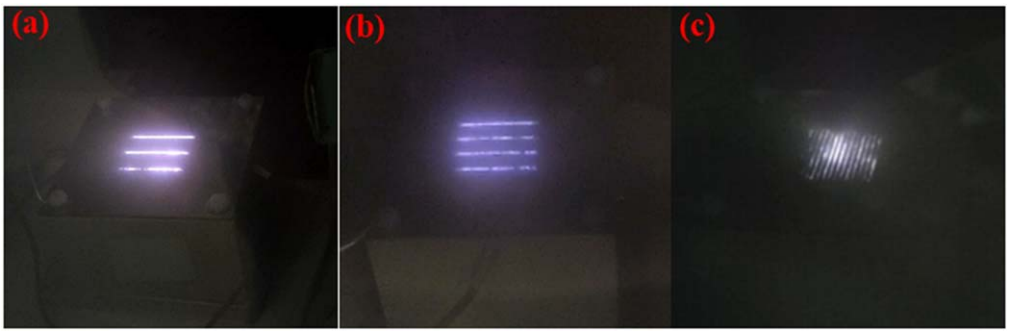

Figure 9. Ignition diagrams of thrusters. (a) −3800 V, (b) −3800 V, (c) −4500 V.

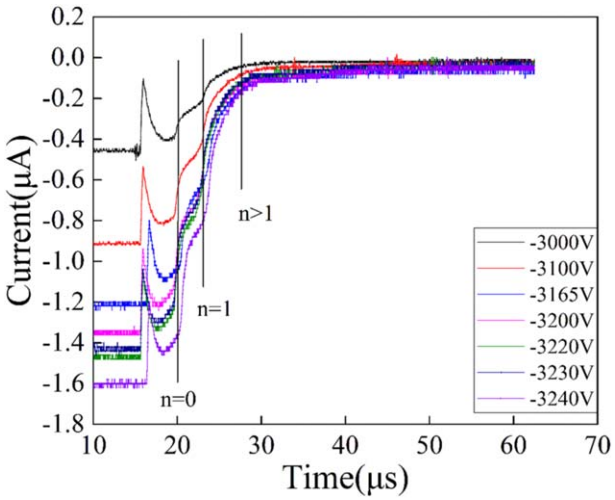

Figure 10. TOF data with 3 emitter-strips at different extraction voltages.

Table 2. The average proportion of each ion cluster in the plumes with 3 emitter-strips.

Propellant	$(EMI-BF_4)_nBF_4^-$		
Number of molecules	$n=0$	$n=1$	$n>1$
Average proportion (%)	35.32	37.19	27.49

According to table 2, specific impulse and thrust are shown at different extraction voltages in figure 13. The thruster can achieve thrust of 4.9–219.2 μN with specific impulse of 4409–5047 s at −2900 to −3800 V. The performance of the thruster was similar to that of 1 strip thruster, and the specific impulse increased with the increase of extraction voltage. The thrust and emission current increased exponentially as the extraction voltage increasing, and then increased linearly.

5. Conclusion

In this study, the emitter of electrospray thruster adopted a strip structure, and ignition experiments were carried out on thrusters

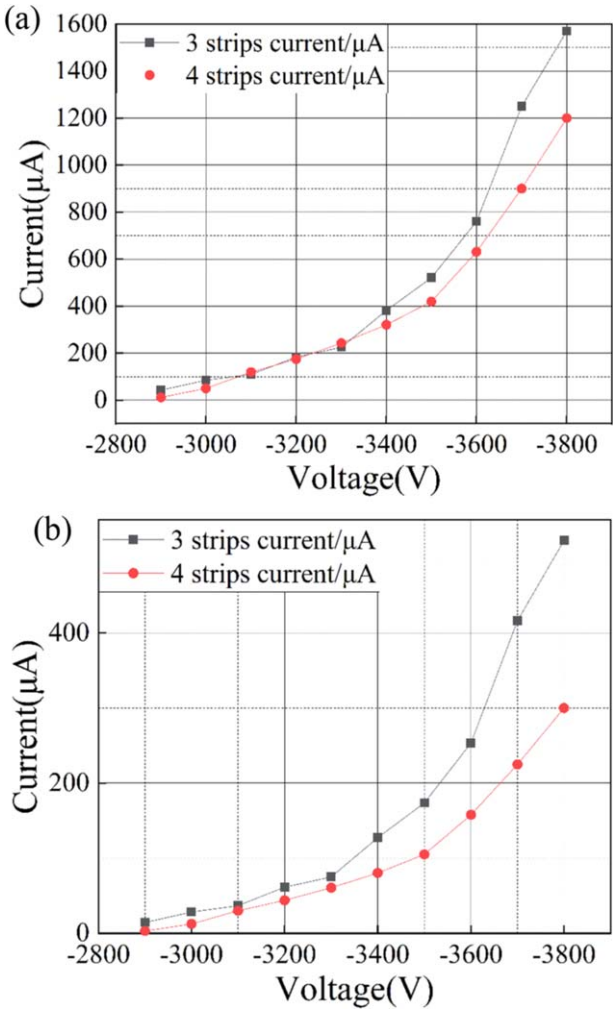

Figure 11. (a) Trend of total emission currents changing with extraction voltages, (b) emission currents per strip at different extraction voltages.

with 1, 3, 4 and 14 emitter-strips. Volt-ampere characteristics with different number of emitter-strips were obtained, and all four types of thrusters achieved reliable ignition. The number of strips (on the emission surface of same size, 4 cm^2) affected stable operational state of the thruster. It can operate stably for a long time of 1, 3 and 4 emitter-strips. According to the experimental results, the maximum extraction voltage, and emission current of the four thrusters are different under stable operational conditions.

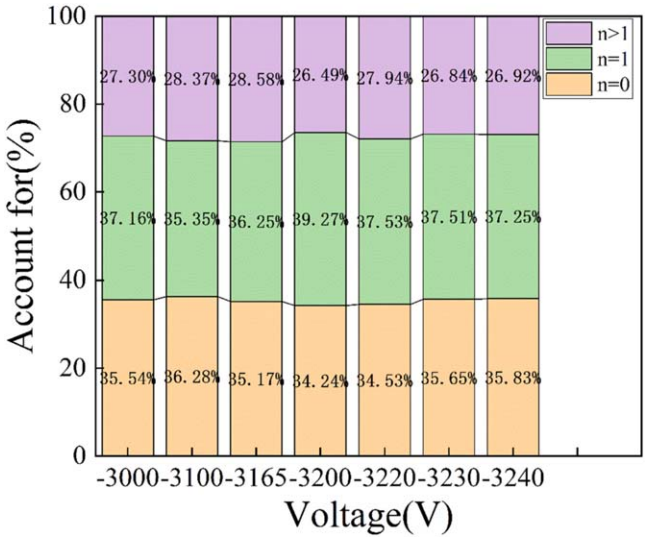

Figure 12. Proportion of plume components with 3 emitter-strips.

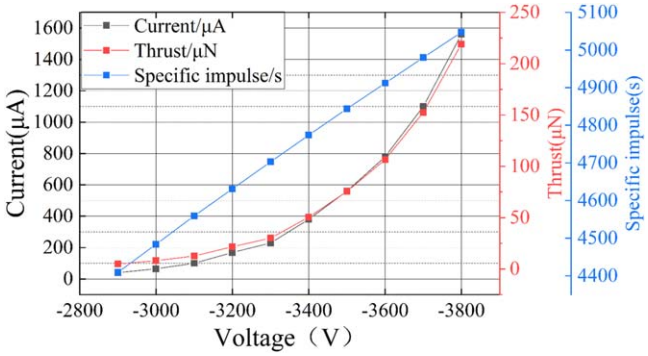

Figure 13. Emission current, thrust and specific impulse with 3 emitter-strips.

The measured stable emission currents and extraction voltages were −500 μA/−5000 V, −1570 μA/−3800 V, −1200 μA/−3800 V and −650 μA/−4500 V, respectively. Increasing the number of strips may not result in the emission current increasing, but changing the stable operational range of the emission current per strip and the extraction voltage. The maximum stable operational extraction voltages of 3 and 4 emitter-strips are lower than those of 1 and 14 emitter-strips, but the emission currents are higher than those of 1 and 14 emitter-strips. TOF was used in the experiment to analyze plume compositions of 1 and 3 emitter-strips, and the total proportions (BF_4^- plus $(EMI-BF_4)BF_4^-$) were about 72.68% and 72.51%, respectively. Also, the effect of the number of strips and extraction voltage on the plume composition was particularly small. Their thrusts were 80.1 μN, 219.2 μN with specific impulses of 5774 s, 5047 s, respectively.

ORCID iDs

Chong CHEN (陈冲) https://orcid.org/0000-0003-2092-3614

References

[1] Rosell-Llompart J, Grifoll J and Loscertales I G 2018 *J. Aerosol Sci.* **125** 2
[2] Rayleigh L 1882 *London, Edinburgh Dublin Phil. Mag. J. Sci.* **14** 184
[3] Taylor G 1964 *Proc. R. Soc.* A **280** 383
[4] Krejci D and Lozano P 2016 Scalable ionic liquid electrospray thrusters for nanosatellites *Proc. 39th Annual AAS Guidance and Control Conf. (Breckenridge, Colorado, USA, 5–10 February 2016)*
[5] Krejci D and Lozano P 2017 Micro-machined ionic liquid electrospray thrusters for Cubesat applications *Proc. 35th Int. Electric Propulsion Conf. (Atlanta, Georgia, USA, 8–12 October 2017)*
[6] Krejci D *et al* 2017 *J. Spacecr. Rockets* **54** 447
[7] Lozano P and Martínez-Sánchez M 2004 *J. Colloid Interface Sci.* **280** 149
[8] Brikner N and Lozano P C 2012 *Appl. Phys. Lett.* **101** 193504
[9] Lozano P C *et al* 2015 *MRS Bull.* **40** 842
[10] Courtney D G, Li H Q and Lozano P 2012 *J. Phys. D: Appl. Phys.* **45** 485203
[11] Legge R S Jr and Lozano P C 2011 *J. Propul. Power* **27** 485
[12] Guerra-Garcia C, Krejci D and Lozano P 2016 *J. Phys. D: Appl. Phys.* **49** 115503
[13] Ma C and Ryan C 2019 Plume characterization of a porous electrospray thruster *Proc. 36th Int. Electric Propulsion Conf. (Vienna, Austria, 15–20 September 2019)*
[14] Mitterauer J 1987 *IEEE Trans. Plasma Sci.* **15** 593
[15] Marcuccio S, Giusti N and Tolstoguzov A 2009 Characterization of linear slit FEEP using a ionic liquid propellant *Proc. 31st Int. Electric Propulsion Conf. (Ann Arbor, Michigan, USA, 20–24 September 2009)*
[16] Marcuccio S, Pergola P and Giusti N 2012 A simplified, low cost electric thruster for micro- and nano-satellites *Proc. Small Satellites Systems and Services (4S) Symp. (Portorose, Slovenia, 2012)*
[17] Courtney D G, Dandavino S and Shea H 2016 *J. Propuls. Power* **32** 392
[18] Courtney D G, Alvarez N and Demmons N R 2018 Electrospray thrusters for small spacecraft control pulsed and steady state operation *Proc. 2018 Joint Propulsion Conf. (Cincinnati, Ohio, 9–11 July 2018)*
[19] Courtney D G 2019 High-speed transient characterization of the busek BET-300-P electrospray thruster *Proc. 36th Int. Electric Propulsion Conf. (Vienna, Austria, 15–20 September 2019)*
[20] Chen C, Chen M L and Zhou H H 2020 *Plasma Sci. Technol.* **22** 094009
[21] Chen C *et al* 2021 *Acta Astronaut.* **178** 192